

Dynamic amplification in a periodic structure subject to a moving load passing a transition zone: Hyperloop case study

Faragau, A.B.; Metrikine, A.; van Dalen, K.N.

DOI

[10.1007/978-3-031-15758-5_67](https://doi.org/10.1007/978-3-031-15758-5_67)

Publication date

2022

Document Version

Final published version

Published in

Recent Trends In Wave Mechanics and Vibrations

Citation (APA)

Faragau, A. B., Metrikine, A., & van Dalen, K. N. (2022). Dynamic amplification in a periodic structure subject to a moving load passing a transition zone: Hyperloop case study. In Z. Dimitrovová, R. Gonçalves, P. Biswas, & T. Silva (Eds.), *Recent Trends In Wave Mechanics and Vibrations: Proceedings of WMVC 2022* (pp. 651-661). (Mechanisms and Machine Science; Vol. 125). Springer. https://doi.org/10.1007/978-3-031-15758-5_67

Important note

To cite this publication, please use the final published version (if applicable).
Please check the document version above.

Copyright

Other than for strictly personal use, it is not permitted to download, forward or distribute the text or part of it, without the consent of the author(s) and/or copyright holder(s), unless the work is under an open content license such as Creative Commons.

Takedown policy

Please contact us and provide details if you believe this document breaches copyrights.
We will remove access to the work immediately and investigate your claim.

Green Open Access added to TU Delft Institutional Repository

'You share, we take care!' - Taverne project

<https://www.openaccess.nl/en/you-share-we-take-care>

Otherwise as indicated in the copyright section: the publisher is the copyright holder of this work and the author uses the Dutch legislation to make this work public.

Mechanisms and Machine Science

Zuzana Dimitrovová
Paritosh Biswas
Rodrigo Gonçalves
Tiago Silva *Editors*

Recent Trends in Wave Mechanics and Vibrations

Proceedings of WMVC 2022



 Springer

Zuzana Dimitrovová · Paritosh Biswas ·
Rodrigo Gonçalves · Tiago Silva
Editors

Recent Trends in Wave Mechanics and Vibrations

Proceedings of WMVC 2022

Editors

Zuzana Dimitrovová
Departamento de Engenharia Civil
Universidade Nova de Lisboa
Caparica, Portugal

IDMEC, Instituto Superior Técnico
Universidade de Lisboa
Lisbon, Portugal

Rodrigo Gonçalves
Departamento de Engenharia Civil
Universidade Nova de Lisboa
Caparica, Portugal

Paritosh Biswas
University of North Bengal
Jalpaiguri, West Bengal, India

Tiago Silva
Depart. de Eng Mecânica e Industrial
Universidade Nova de Lisboa
Caparica, Portugal

ISSN 2211-0984

Mechanisms and Machine Science

ISBN 978-3-031-15757-8

<https://doi.org/10.1007/978-3-031-15758-5>

ISSN 2211-0992 (electronic)

ISBN 978-3-031-15758-5 (eBook)

© The Editor(s) (if applicable) and The Author(s), under exclusive license
to Springer Nature Switzerland AG 2023

This work is subject to copyright. All rights are solely and exclusively licensed by the Publisher, whether the whole or part of the material is concerned, specifically the rights of translation, reprinting, reuse of illustrations, recitation, broadcasting, reproduction on microfilms or in any other physical way, and transmission or information storage and retrieval, electronic adaptation, computer software, or by similar or dissimilar methodology now known or hereafter developed.

The use of general descriptive names, registered names, trademarks, service marks, etc. in this publication does not imply, even in the absence of a specific statement, that such names are exempt from the relevant protective laws and regulations and therefore free for general use.

The publisher, the authors, and the editors are safe to assume that the advice and information in this book are believed to be true and accurate at the date of publication. Neither the publisher nor the authors or the editors give a warranty, expressed or implied, with respect to the material contained herein or for any errors or omissions that may have been made. The publisher remains neutral with regard to jurisdictional claims in published maps and institutional affiliations.

This Springer imprint is published by the registered company Springer Nature Switzerland AG
The registered company address is: Gewerbestrasse 11, 6330 Cham, Switzerland



Dynamic Amplification in a Periodic Structure Subject to a Moving Load Passing a Transition Zone: Hyperloop Case Study

Andrei B. Fărăgău^(✉), Andrei V. Metrikine, and Karel N. van Dalen

Delft University of Technology, Stevinweg 1, 2628, CN Delft, The Netherlands
A.B.Faragau@tudelft.nl

Abstract. Hyperloop is an emerging high-speed transportation system in which air resistance is minimised by having the vehicle travel inside a de-pressurised tube supported by columns. This design leads to a strong *periodic* variation of the stiffness (among other parameters) experienced by the vehicle. Also, along its route, the Hyperloop will encounter so-called *transition zones* (e.g., junctions, bridges, etc.), where the properties (e.g., support stiffness) are different than for the rest of the structure. In railway engineering, increased degradation is seen in the vicinity of these transition zones, leading to increased frequency of maintenance. This work investigates response amplification mechanisms in a Hyperloop system that arise due to the combination of a transition zone and the structure having a periodic nature. The amplification mechanisms investigated here can help prevent degradation of the Hyperloop tube close to transition zones as well as fatigue and wear of the vehicle.

Keywords: Periodic structure · Moving load · Hyperloop · Transition radiation · Wave interference

1 Introduction

Periodic systems under the action of moving loads have been extensively studied by researchers in the past century. These problems do not only pose academic challenges but are also of high practical relevance due to their application in railway, road, and bridge engineering, among others. Despite numerous studies on periodic systems (e.g., [1, 2]), only few of them investigate the influence of a local inhomogeneous region, a so-called transition zone, on the dynamic response. In railway and road engineering, increased degradation is seen in the vicinity of these transition zones [3–6], leading to increased maintenance requirements.

Hyperloop is a new emerging transportation system that is in the development stage. Its design minimises the air resistance by having the vehicle travel inside a de-pressurised tube (near vacuum) supported by columns. This design

may lead to a strong periodic variation of the stiffness experienced by the vehicle. Moreover, along its route, it will cross bodies of water or come across junctions/switches, all of which are transition zones.

The current study investigates the potential response amplification in a Hyperloop system that results from the combination of (i) a transition zone and (ii) the structure having a periodic nature. In a previous study [7], three such phenomena have been identified in a system representative of a catenary structure (overhead wires in railway tracks). In this work, the three phenomena identified in Ref. [7] are investigated using a model representative for a Hyperloop transportation system. Accounting for these phenomena in the design can help prevent degradation of the Hyperloop tube close to transition zones as well as fatigue and wear of the transportation pod.

2 Model Description and Solution Method

The system formulated here consists of an infinite Euler-Bernoulli beam with mass per unit length ρ , bending stiffness EI , and material damping ratio ζ . The beam is discretely supported by springs with stiffness $k_s(x)$ and dashpots with damping coefficient $c_s(x)$, and a point mass m_s is located at each support. $x \in [nd, (n+1)d]$ is the generic cell where n is the cell number and d is the cell width, and the spring-dashpot-mass element is located in the middle of the cell at $x = \bar{n}d$ with $\bar{n} = n + \frac{1}{2}$. The system is acted upon by a moving constant load of amplitude F_0 and velocity v . A zone (stiff zone) of length l has the stiffness and damping of the supports p times larger than for the rest of the infinite domain; the region covering the stiff zone and its close vicinity is called the transition zone. Figure 1 visually describes the system, while its equation of motion reads

$$EI(1+\zeta \frac{\partial}{\partial t})w'''' + \rho \ddot{w} + \sum_{n=-\infty}^{\infty} \left(m_s \frac{\partial^2}{\partial t^2} + c_s(x) \frac{\partial}{\partial t} + k_s(x) \right) w \delta(x - \bar{n}d) = -F_0 \delta(x - vt), \quad (1)$$

where primes and overdots denote partial derivatives in space and time, respectively. The stiffness $k_s(x)$ is a piecewise-defined function in space and it reads

$$k_s(x) = \begin{cases} k_s, & x < x_a, \\ p k_s, & x_a \leq x \leq x_b, \\ k_s, & x > x_b. \end{cases} \quad (2)$$

For simplicity, the same spatial distribution is assumed for the damping.

There are multiple designs of the Hyperloop transportation system; here, a typical Hyperloop design is considered. The steel tube has a thickness of 19 mm and an inner diameter of 2.5 m, leading to $\rho = 1331$ kg/m (a 10% increase was considered to account for additional equipment) and $EI = 2.5 \times 10^{10}$ Nm². The support stiffness is tuned using a FEM analysis of the 3D structure (excluding the soil) such that the displacement at the location of the supports match when a static load is applied in the middle of the span. Note that the displacement

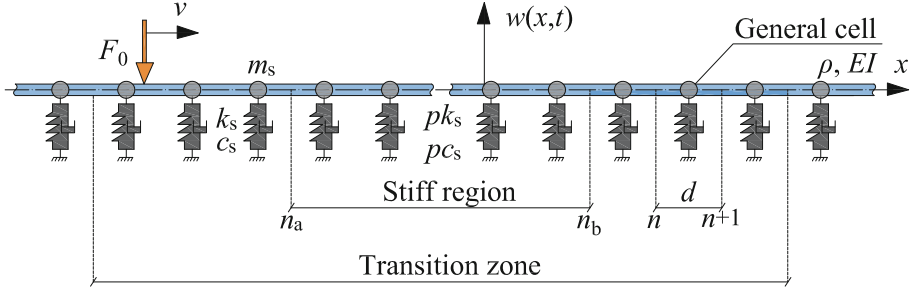


Fig. 1. Model schematics: infinite Euler-Bernoulli beam discretely supported by an inhomogeneous foundation, subjected to a moving constant load.

is at the rail level which is located at the top of the tube (the vehicle is suspended from the top in this design); therefore, the stiffness of the support (in our phenomenological model) accounts not only for the stiffness of the column, but also for the flexibility of the connection between the tube and the rail and, most importantly, for the flexibility introduced by the ovalization of the tube. The concrete columns supporting the tube have a spacing of $d = 16$ m and are assumed to be of 1.5 m diameter and 5 m height; the point mass in the model represents the mass of the columns that is activated by the vehicle and is chosen here as 10% of the overall mass of the column $m_s = 2332$ kg (such a small value is chosen because most flexibility at the supports comes from the ovalization of the tube and thus, the columns are not deformed much). When it comes to the damping, a very small amount is assumed to be conservative, namely $\zeta = 5 \times 10^{-6}$ and $c_s = 10$ kNs/m. Although the damping seems small, it originates mostly from the tube itself and not from the soil (since the columns are not deformed much) and the metal tube is not expected to have high damping.

2.1 Solution Method for the Homogeneous System

The approach to determine the steady-state solution for the system without a transition zone is based on the Floquet theory [8]. The procedure is explained in detail for a string in Ref. [7] and is summarized in the following. After applying the Fourier transform over time to Eq. (1), the analysis can be restricted to one cell without loss of generality. The relation between the states (displacement, slope, bending moment, and shear force) at the two boundaries of the generalized cell reads (see [7] for a detailed derivation)

$$\tilde{\mathbf{w}}_{n+1} = \mathbf{F}\tilde{\mathbf{w}}_n + \tilde{\mathbf{w}}_{n+1}^{\text{ML}}, \quad (3)$$

where the 4×4 matrix \mathbf{F} is the Floquet matrix and $\tilde{\mathbf{w}}_{n+1}^{\text{ML}}$ includes the influence of the particular solution to the equation of motion. Performing the eigenvalue (α) and eigenvector (\mathbf{u}) decomposition of \mathbf{F} leads to the following expression:

$$\tilde{\mathbf{w}}_n = a_1 e^{-ik_1^F nd} \mathbf{u}_1 + a_2 e^{-ik_2^F nd} \mathbf{u}_2 + a_3 e^{-ik_3^F nd} \mathbf{u}_3 + a_4 e^{-ik_4^F nd} \mathbf{u}_4 + \tilde{\mathbf{w}}_{n+1}^{\text{ML}}, \quad (4)$$

where a_1, a_2, a_3 , and a_4 are unknown amplitudes and $k^F = \frac{i \ln(\alpha)}{d}$ are the Floquet wavenumbers. To fully determine the solution, the so-called *periodicity condition* [7,9] is used, which imposes the response inside each cell to be exactly the same as in the previous one but shifted in time by $\frac{d}{v}$. The periodicity condition leads to four conditions (displacement, slope, moment, and shear force) with which all four unknown amplitudes are determined. The steady-state solution in the Fourier domain is now determined, and to obtain the time-domain solution, the inverse Fourier transform is performed numerically.

The dispersion characteristics of the system without the transition zone are presented in Fig. 2. There are infinitely many wavenumbers k^F corresponding to one frequency ω and the distance between subsequent wavenumbers is $\frac{2\pi}{d}$. These repeating zones are called Brillouin zones [10] (just three zones are presented in Fig. 2, but there are infinitely many). For discrete systems, all information about wave propagation is contained in the first Brillouin zone. Unlike discrete systems, continuous ones allow for wave propagation at all wavenumbers. Consequently, the response $\tilde{w}(x, \omega)$ will contain wavenumbers from all Brillouin zones and the continuous wavenumber reads $k = k^F + m \frac{2\pi}{d}$ with $m = \pm 1, \pm 2, \dots$. Also, Fig. 2 shows that the periodic system exhibits multiple (actually infinitely many [10]) frequency ranges where no propagation is possible; these frequency ranges are called *stop bands*, while the frequency ranges in which propagation is possible are called *pass bands*. Strictly speaking, stop/pass bands only exist if the system does not have dissipation; however, for small values of dissipation, the wave propagation is strongly attenuated in the stop bands.

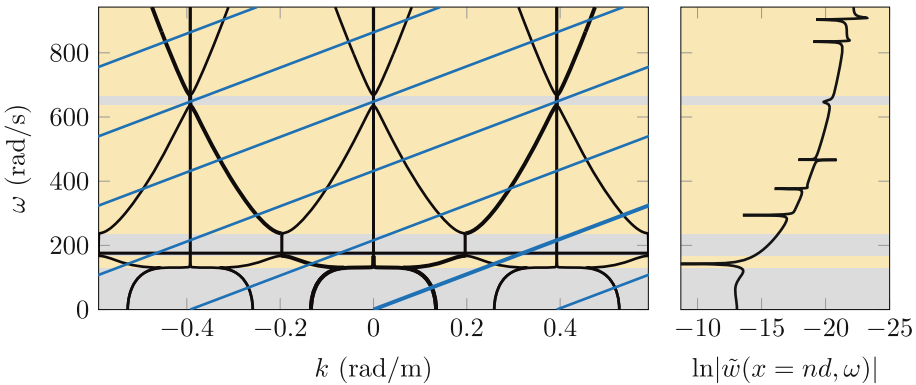


Fig. 2. The dispersion curves in three Brillouin zones (black lines) and the kinematic invariants (blue lines) (left panel), and the frequency spectrum of the steady-state displacement (right panel); the grey/yellow background represents a stop/pass band.

To determine the frequency and wavenumbers of the waves generated by the moving load, we need another equation next to the dispersion equation that expresses a relation between the frequency, wavenumber, and the load velocity,

namely the kinematic invariant. There are infinitely many kinematic invariants (seven of them are presented in Fig. 2). The 0th-order kinematic invariant is given by $\omega = kv$ while the higher order kinematic invariants are given by $\omega = kv + m \frac{2\pi v}{d}$ with $m = \pm 1, \pm 2, \dots$. The intersections between one of the kinematic invariants and the dispersion curve represent waves emitted by the moving load in the steady state, as can be seen in the right panel of Fig. 2. Moreover, it is important to observe that the emitted waves form a discrete frequency spectrum and that all generated waves have frequencies in the pass bands of the system.

2.2 Solution Method for the Inhomogeneous System

The transient solution is obtained by firstly determining the response of the system to the moving load acting inside each individual cell separately, and then superimposing the individual solutions. To determine the response of the system to the moving load acting inside only one cell, the forward Fourier transform is applied over time to Eq. (1). The obtained equation of motion is then divided in 5 domains; when, for example, the moving load is applied to the left of the stiff zone, the 5 domains are (1) left of the loaded cell, (2) the loaded cell, (3) right of the loaded cell and left of the stiff zone, (4) inside the stiff zone, and (5) to the right of the stiff zone. When the moving load is applied to the stiff zone or to the right of the stiff zone, an analogous division is made. The solutions of the 5 domains are analogous to Eq. (4) where $\tilde{\mathbf{w}}_{n+1}^{\text{ML}}$ appears only in the loaded domain. The 5 solutions have 16 unknown amplitudes (after applying the boundary conditions at infinite distance from the load), which are determined from the interface conditions between the domains (i.e., continuity in displacements, slopes, bending moments, and shear forces). This procedure is repeated until the moving load is applied inside each individual cell of interest.

To obtain the response of the system to the moving load acting on all cells, the individual solutions are superimposed as follows:

$$\tilde{\mathbf{w}}_n = \sum_{n_\xi=N_{\text{left}}}^{N_{\text{right}}} \tilde{\mathbf{w}}_{n,n_\xi}, \quad (5)$$

where $\tilde{\mathbf{w}}_{n,n_\xi} = [\tilde{\mathbf{w}}_{1,n,n_\xi}, \tilde{\mathbf{w}}_{2,n,n_\xi}, \tilde{\mathbf{w}}_{3,n,n_\xi}, \tilde{\mathbf{w}}_{4,n,n_\xi}, \tilde{\mathbf{w}}_{5,n,n_\xi}]$ is the solution for all the cells when the load is applied at n_ξ , N_{left} is the first cell on which the load acts (at $t = 0$) and N_{right} represents the last cell. N_{left} needs to be chosen sufficiently to the left of the transition zone such that the response is in the steady state prior to reaching the transition zone. N_{right} can be chosen based on the maximum time of the simulation and it does not introduce any unwanted transients in the response. The solution is now determined at the interfaces between cells. To determine the solution inside the cells, one needs to use the equations that lead to the Floquet matrix (see Eq. (8) in [7]).

Next, three phenomena that lead to amplifications of the response in the transition zone are investigated.

3 Wave Interference Phenomenon

The increased support stiffness of the stiff zone causes an upward shift in frequency of its stop bands compared to the soft zones. Consequently, a wave generated by the moving load outside the transition zone can be reflected at the stiff region provided that the frequency of the wave is in a stop band of the stiff region. This leads to wave interference between the reflected wave and the wave field radiated by the approaching load, which in turn can cause an amplification of the response in the transition zone.

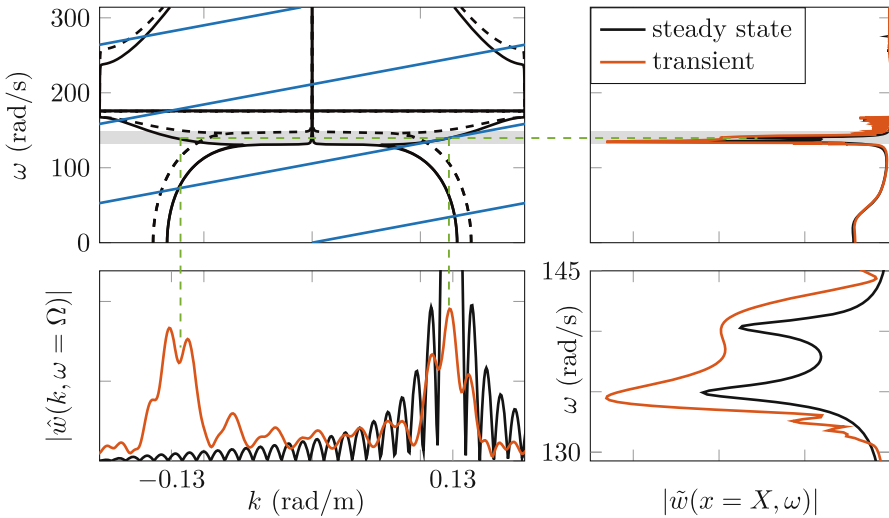


Fig. 3. The dispersion curves for the soft (black solid line) and stiff (black dashed line) regions and the kinematic invariants (blue lines) (top left panel), the displacements frequency spectra to the left of the stiff zone (top right panel; $X = x_a - 5$ m), and the wavenumber spectra of the displacements (bottom left panel) evaluated at $\Omega = 140$ rad/s (indicated by the horizontal green dashed line); the bottom right panel is a zoom in of the top right panel; the grey background indicates the overlapping region of the pass-band of the soft zone and the stop-band of the stiff one; $p = 1.3$ and $v = 269$ m/s.

The frequency-domain response in Fig. 3 shows that there are two harmonics of large amplitude generated in the steady state, which are in one of the stop-bands of the stiff zone. These waves are, as can be seen, amplified in the transient response (at the left of the stiff zone) due to the wave interference between the incoming and reflected waves. The reflection of one of the two harmonics (the one at $\omega = 140$ rad/s) can be seen in the wavenumber-domain response through the presence of an additional peak (compared to the steady state) at wavenumber equal in magnitude but opposite in sign (i.e., opposite direction of propagation) to that of the forward propagating wave.

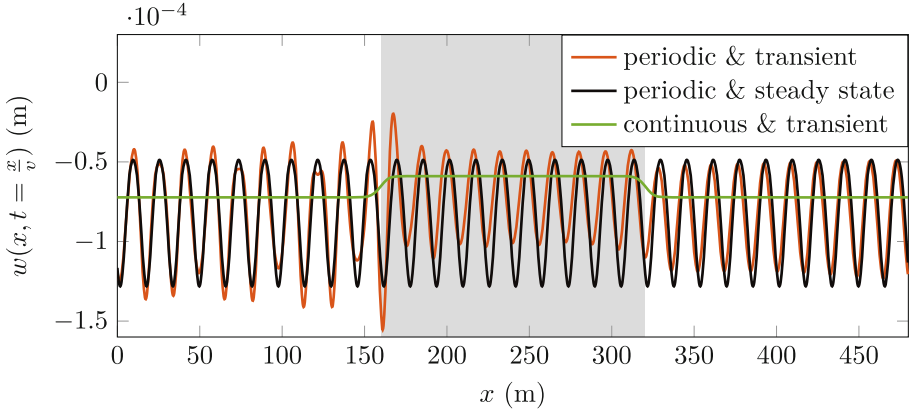


Fig. 4. The displacement evaluated under the moving load for the wave-interference phenomenon; the location of the stiff zone is indicated by the grey background.

To quantify the amplification, the time-domain response under the moving load is presented in Fig. 4. The response is evaluated under the moving load because it is governing. A considerable amplification can be observed at the left of the stiff zone that, at its maximum, is of about 20%. The response of the equivalent continuously supported system with a transition zone is also presented to show that, in that case, there is no visible amplification. Clearly, this significant amplification is caused by the periodicity of the system together with the transition zone; if any of these two characteristics are removed, the amplification vanishes.

It is important to note that a larger difference in stiffness p does not cause a significant increase in the amplification; the important factor for this phenomenon is that p is such that the generated harmonics are in one of the stop bands of the stiff zone. Also, even though the velocity is in the operational range for Hyperloop, it is chosen specifically for this mechanism to occur (see Sect. 4.1 in Ref. [7] for the choice of velocity); for other velocities, the generated waves are either of low amplitude or inside the pass-bands of the stiff zone, making this mechanism not to occur. Finally, the larger the damping (especially the tube's internal damping), the smaller the amplification observed because the generated waves cannot propagate sufficiently far before being attenuated.

4 Passing from Non-resonance Velocity to a Resonance Velocity

The velocity at which one of the kinematic invariants is tangential to one of the dispersion curves is called critical velocity. At such velocities, resonance of the system occurs. From a physical point of view, resonance occurs because the group velocity of the generated wave is equal to the load velocity, which makes

that the wave cannot propagate away and leads to a build up of energy around the moving load.

The properties of the Hyperloop system should be chosen such that these resonance velocities are far away from operational speeds. However, even if the operational velocity is far from resonance velocities outside transition zones, it can be close to a resonance velocity inside it. In this section, we investigate the situation in which the load passes from non-resonance velocity in the soft region to a resonance velocity inside the stiff region. Note that the load velocity is kept constant and the resonance velocity just changes due to higher support stiffness.

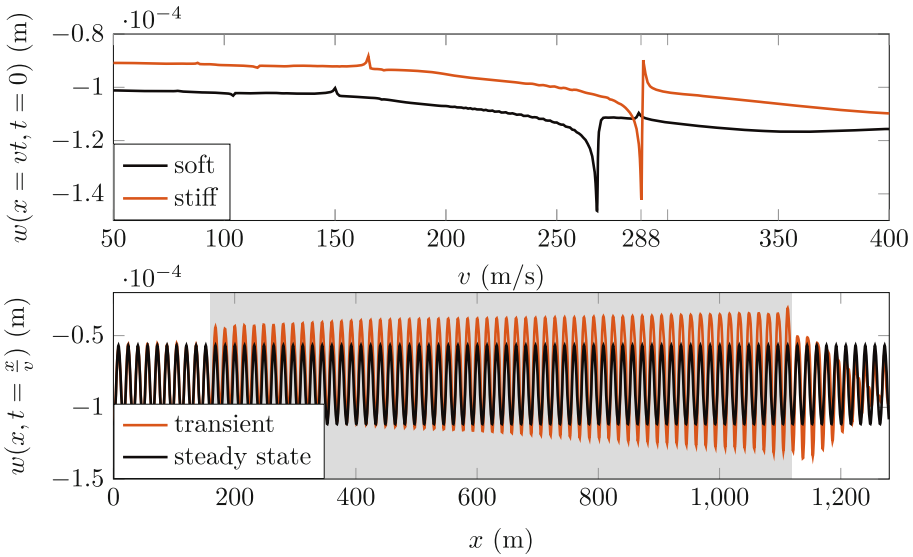


Fig. 5. Response under the load vs velocity in the soft and stiff regions (top panel) and the displacements evaluated under the moving load for resonance in the stiff zone (bottom panel); the stiff zone is marked by the grey background; $p = 1.3$.

The top panel in Fig. 5 presents the resonance velocities for the soft and stiff regions. For $v \approx 288$ m/s, the stiff zone resonates while the soft one does not. The bottom panel in Fig. 5 presents the displacement under the moving load for $v = 288$ m/s. The amplification in the stiff zone is clearly observed with a drastic increase compared to the steady state. At its maximum, the amplification of the displacement is of more than 20% while the amplification of the bending moment (not presented here for brevity) is more than 25%. The increase in response requires many cell lengths to develop, characteristic to resonance; for short stiff zones, resonance might not have time to develop, but for longer ones strong response amplification can develop. It must be mentioned that increasing the damping diminishes the amplification, as expected for resonance.

5 Wave Trapping Inside the Stiff Zone

The stiff zone has a finite length l , and consequently the incoming waves generated by the moving load in the soft region could get trapped inside. Wave trapping could lead to response amplification inside the stiff zone even when the moving load is relatively far away. The conditions for a wave to get trapped in the stiff zone are described in detail in Ref. [7] and are summarized in the following. An approximate condition for wave trapping is that q half-wavelengths of the wave inside the stiff zone is equal to or an integer fraction of l . From this conditions, the wavenumber k_{tr} of the wave trapped in the stiff zone can be determined, and from the dispersion curves (Fig. 2 with the properties of the stiff zone), the corresponding frequency ω_{tr} can be obtained. The incoming wave from the soft zone needs to have the same frequency ω_{tr} and the corresponding wavenumber $k_{tr,2}$ can be determined from the dispersion curves with the properties of the soft zone. So, the incoming wave from the soft zone with wavenumber $k_{tr,2}$ and frequency ω_{tr} will lead to a wave of wavenumber k_{tr} and frequency ω_{tr} in the stiff zone that will get trapped. The load velocity that excites a wave of wavenumber $k_{tr,2}$ and frequency ω_{tr} can be obtained from the kinematic invariant expression.

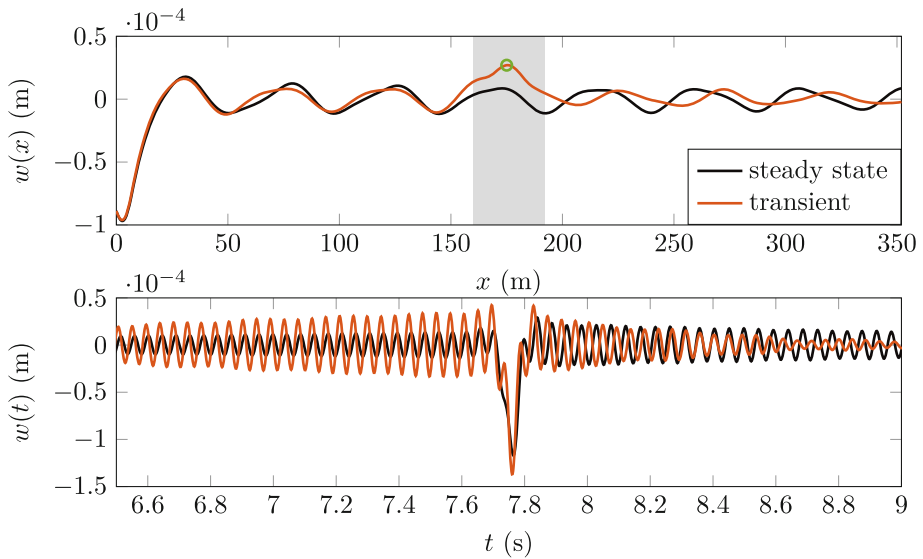


Fig. 6. Snapshot of the time-domain displacements (top panel) and the displacements time-history at the point marked by the green circle (bottom panel) for the situation when the wave is trapped in the stiff zone; the stiff zone is indicated by the grey background; $p = 1.2$ and $v = 270$ m/s.

The top panel in Fig. 6 presents a snapshot of the displacement field where the trapped wave can be clearly observed even though the load is relatively

far away. The bottom panel in Fig. 6 presents the displacement time-history at a point inside the stiff zone. The amplitude inside the stiff zone is more than double the one of the steady state when the load is relatively far away from the transition zone; under the moving load, at its maximum, the amplification is around 17%. For slightly different velocities or different lengths of the stiff zone (except for integer fractions of half the wavelength), the amplification vanishes.

6 Conclusions

This paper investigated three phenomena that can lead to response amplification in a continuous and periodic system with a transition zone (described by an increase in support stiffness); the system is representative of a Hyperloop transportation system. The phenomena are the product of a periodic system and a local inhomogeneity, and if one of these characteristics is omitted, the phenomena will not occur.

The wave-interference phenomenon leads to response amplification at the edges of the stiff zone while the passing-to-critical-velocity and wave-trapping phenomena cause amplification inside the stiff zone. While the wave-interference and wave-trapping phenomena lead to response amplification also for short transition zones, the passing-to-critical-velocity requires a long stiff zone for the amplification to develop. Results show that all three phenomena can lead to a response amplification which, at its maximum, is about 20%. Also, the phenomena have been observed at envisioned operational velocities of the Hyperloop vehicles.

Although this amplification would not cause failure of the structure, over time it can lead to increased degradation of the structure as well as discomfort for passengers. Moreover, all three phenomena are diminished with increased damping; therefore, if the designed system does not have sufficient inherent damping, additional passive or active damping measures may be needed. Finally, the three investigated phenomena can be considered as additional constraints for the design parameters at transition zones such that amplifications are avoided.

Acknowledgements. This research is supported by the Dutch Technology Foundation TTW [Project 15968], part of the Netherlands Organisation for Scientific Research (NWO), and which is partly funded by the Ministry of Economic Affairs.

References

1. Mead, D.J.: Wave propagation in continuous periodic structures: research contributions from southampton. *J. Sound Vib.* **190**, 495–524 (1996)
2. Jezequel, L.: Response of periodic systems to a moving load. *J. Appl. Mech. Trans. ASME* **48**(3), 613–618 (1981)
3. Steenbergen, M.J.M.M.: Physics of railroad degradation: The role of a varying dynamic stiffness and transition radiation processes. *Comput. Struct.* **124**, 102–111 (2013)

4. Fărăgău, A.B., Metrikine, A.V., van Dalen, K.N.: Transition radiation in a piecewise-linear and infinite one-dimensional structure-a Laplace transform method. *Nonlinear Dyn.* **98**, 2435–2461 (2019)
5. Fărăgău, A.B., Mazilu, T., Metrikine, A.V., Lu, T., van Dalen, K.N.: Transition radiation in an infinite one-dimensional structure interacting with a moving oscillator-the Green's function method. *J. Sound Vibration* **492** (2021)
6. Fărăgău, A.B., Keijndener, C., de Oliveira Barbosa, J.M., Metrikine, A.V., van Dalen, K.N.: Transition radiation in a nonlinear and infinite one-dimensional structure: a comparison of solution methods. *Nonlinear Dyn.* **103**(2), 1365–1391 (2021). <https://doi.org/10.1007/s11071-020-06117-0>
7. Fărăgău, A.B., de Oliveira Barbosa, J.M., Metrikine, A.V., van Dalen, K.N.: Dynamic amplification in a periodic structure with a transition zone subject to a moving load: three different phenomena. *Math. Mech. Solids* **27**(9), 1740–1760 (2022)
8. Floquet, G.: Sur les Equations Differentielles Lineaires a Coefficients Periodiques. *Annales Scientifiques de l'Ecole Normale Supérieure* **12**, 47–88 (1883)
9. Vesnitskii, A.I., Metrikin, A.V.: Transition radiation in mechanics. *Phys. Usp.* **39**(10), 983–1007 (1996)
10. Brillouin, L.: *Wave Propagation in Periodic Structures*. Dover Publications, Inc., ii ed. (1953)